

## Identifying seismogenic EM anomalies in terms of magnetotelluric transfer function

W. Hu<sup>1</sup>, B. Han<sup>2</sup>, X. Chen<sup>2,3</sup>, Y. Fan<sup>2,4</sup> and K. Hu<sup>5</sup>

<sup>1</sup>Key Laboratory of Exploration Technologies for Oil and Gas Resources of MOE, Yangtze University, Wuhan, China. Email: hwb@yangtzeu.edu.cn

<sup>2</sup>State Key Laboratory of Earthquake Dynamics, Institute of Geology, Beijing, China

<sup>3</sup>National Institute of Natural Hazards, Ministry of Emergency Management, Beijing, China

<sup>4</sup>Researcher, China Earthquake Network Center, Beijing, China

<sup>5</sup>Hubei Subsurface Multi-scale Imaging Key Laboratory, School of Geophysics and Geomatics, China University of Geosciences, Wuhan, China

---

### SUMMARY

Data observed by permanent magnetotelluric (MT) stations near earthquake belts have indicated potential seismogenic-induced electromagnetic disturbances. In this paper, an arbitrarily orientated dipole source in layered earth is used to simulate the response of low-frequency pre-earthquake electromagnetic radiation; and parameters of magnetotelluric transfer function are subsequently calculated. Characteristics of frequency, spatial distribution and time-varying of these parameters are analyzed, and the results show possibility of identification of SEM anomalies from observed MT data in seismogenic processes. Long-term MT data from two permanent stations in the Southern segment of South-north Earthquake Belt of China have been processed based on daily variation, and two events of SEM have been identified by comprehensive analysis of multi-parameter anomalies. This study has demonstrated the potential of using subsurface electric dipole simulations for SEM radiation analysis, offering a feasible approach for the prediction and understanding of seismogenic zones by SEM anomalies.

**Keywords:** Seismogenic EM anomaly, MT responses, dipole responses, identifying SEM, EM transfer function

---

### INTRODUCTION

In the study of the natural EM induction in the Earth, the concept of the transfer function is related to the observed stable linear correlation trend of the three geomagnetic field components at many measuring sites. This tendency was first demonstrated by Parkinson (1959) in relation to work off the coast of Australia, and then empirically derived to express the linear relationship between the two horizontal electric-field components ( $E_x$ ,  $E_y$ ) and the three magnetic-field components ( $H_x$ ,  $H_y$  and  $H_z$ ) observed at the earth's surface by MT station. The MT transfer functions are defined (Bastani and Pedersen 2001; Chen 2003) as

$$\begin{bmatrix} E_x \\ E_y \\ H_z \end{bmatrix} = \begin{bmatrix} Z_{xx} & Z_{xy} \\ Z_{yx} & Z_{yy} \\ T_{zx} & T_{zy} \end{bmatrix} \begin{bmatrix} H_x \\ H_y \end{bmatrix} \quad (1)$$

Here the impedance tensor  $\mathbf{Z} = \begin{bmatrix} Z_{xx} & Z_{xy} \\ Z_{yx} & Z_{yy} \end{bmatrix}$  describes the connection between horizontal magnetic and electric fields at a given frequency.

The geomagnetic transfer function (tipper vector)  $\mathbf{T} = \begin{bmatrix} T_{zx} & T_{zy} \end{bmatrix}$  describes the connection between the horizontal and the vertical magnetic-field components.

Both the conventional seismic monitoring networks and permanent MT stations monitor variations of EM fields through continuous observation at fixed points. If a low-frequency electromagnetic radiation is generated during the process of earthquake preparation, the electromagnetic fields recorded by MT station are the superposition of the induced fields generated by natural field source variations and the electromagnetic radiation fields of earthquake preparation underground.

### SIMULATION OF SEM ANOMALIES

The electromagnetic responses of the electric dipole in the horizontally layered earth are calculated using the algorithm by Hu et al. (2023), and the spatial distribution and propagation features of the radiation field and its influence on ground observations have been investigated.

---

EMIW2024 abstracts are distributed under the Creative Commons Attribution 4.0 Unported License. Authors retain the copyright of the abstract but grant any third party the right to use the abstract freely as long as its original authors and citation details are identified.

To view a copy of this license, visit <https://creativecommons.org/licenses/by/4.0/>

**Model**

Set the Cartesian coordinate system with z axis upward and z = 0 km at earth surface; define the angle rotated counterclockwise by the x-axis as the azimuth and the angle rotated clockwise by the z-axis as the inclination. A 5-layered model is designed to simulate the responses of crustal waveguide together with LAI waveguide of the earth, and the model parameters are shown in Figure 1. A conductive cover layer is set to simulate the sediment layer at the earth surface. The vacuum value of permeability ( $\mu_0$ ) and permittivity ( $\epsilon_0$ ) are used for all layers. The excitation source is located in the ground (0, 0, -10 km) as indicated by the red dot of arrow head.

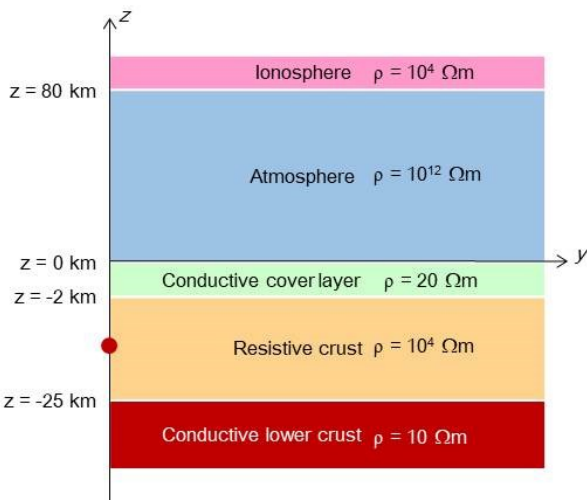


**Figure 1.** Horizontal layered earth model

**Results**

An x-direction inclined electric dipole source (azimuth  $\theta=0^\circ$ , dip angle  $\varphi=30^\circ$ ) is set at a depth of 10 km in a five-layered earth as shown in Figure 1. Figure 2 and 3 show the x-y plane distribution of the apparent resistivity  $\rho_{xy}$  and  $\rho_{yx}$  respectively, derived from two principal elements of the impedance tensor for 100Hz frequency. The white arrow in figure indicates the corresponding location of the electric dipole source in the earth.

It can be seen from Figure 2 that the spatial distribution of the  $\rho_{xy}$  is complex in general. First, the apparent resistivity in the circle shaped neighbor (near-field zone) above the dipole source increases sharply towards the center of the dipole and then decreases slowly away to the dipole center. Second, the apparent resistivity in far-field zone exhibits oscillating pattern as increasing offset, the amplitude of oscillating variation is about  $\pm 50\%$  of the expected surface resistivity, and the spatial period of the oscillation increases with increasing offset. Moreover, along a  $35^\circ$  line from the source

center toward outside, the resistivity is larger than that of the adjacent area, forming a high resistivity strip extending outward, even in far-field region. This indicates that if the station is located near the extension line, large apparent resistivity anomaly can be observed further away from the seismogenic center.

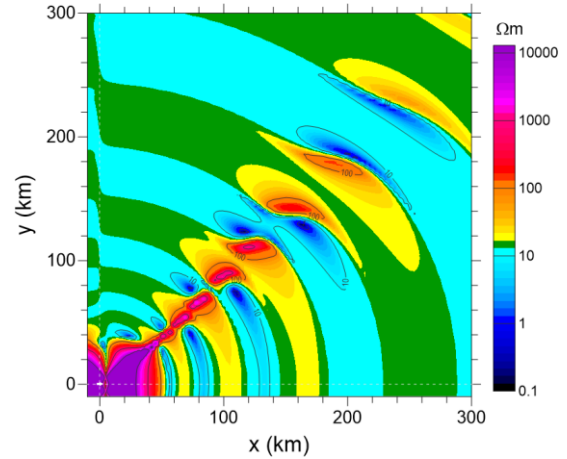


**Figure 2.** Contour plot of  $\rho_{xy}$  at 100Hz in the x-y plane under excitation of an inclined electric dipole source in a five-layer earth.

The spatial distribution pattern of  $\rho_{yx}$  demonstrated in Figure 3 shows similar characteristics as  $\rho_{xy}$  of Figure 2. The main feature of  $\rho_{yx}$  distribution is that more smooth oscillation pattern in the given quadrant with the continuous abnormal strip extending along y-axis. The oscillation has much larger amplitude in the vicinity of the extending abnormal strip.

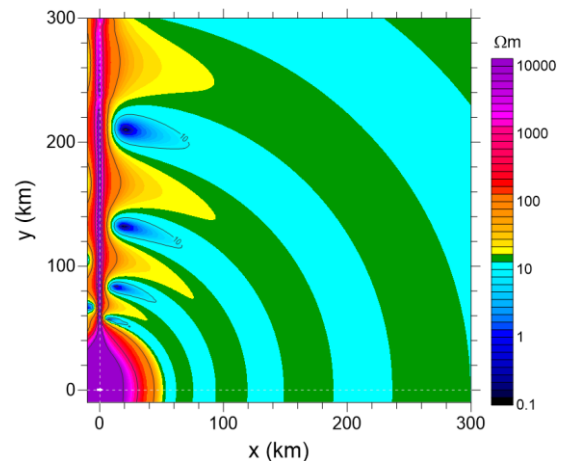


**Figure 3.** Contour plot of  $\rho_{yx}$  at 100Hz in the x-y plane under excitation of an inclined electric dipole source in a five-layer earth.

Figure 4 shows the contour map of tipper ( $T_z$ ) amplitude at 100Hz in the x-y plane under excitation of a  $30^\circ$  tilted electric dipole. The tipper amplitude is calculated from the two elements of tipper vector (induction transfer function). It can be

seen that the amplitude of tipper also show large anomaly in near-field zone and oscillating small anomaly in far-field zone. The maximum amplitude of tipper is 2 according to EM induction theory, thus the oscillating anomaly in far-field zone is really small ( $<0.01$ ), but there are two anomalous strips along both the  $35^\circ$  line and y-axis with relative larger anomaly in the neighboring of these strips.

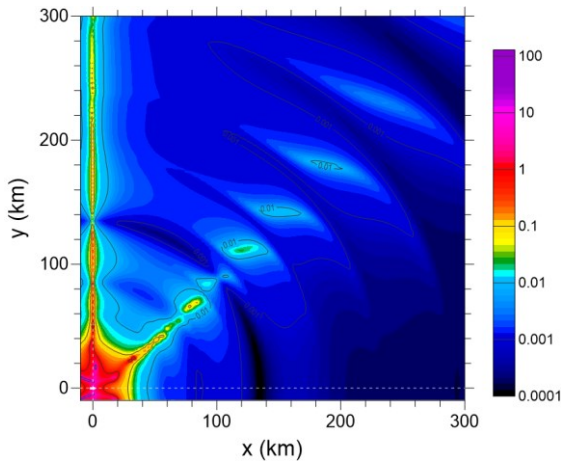


**Figure 4.** Contour plot of  $T_z$  amplitude at 100Hz in the x-y plane under excitation of an inclined electric dipole source in a five-layer earth.

Figure 5 gives the contour view of the azimuth of electric principal axis ( $\theta_p$ ) at 100Hz in the x-y plane under excitation of a  $30^\circ$  tilted electric dipole. The  $\theta_p$  is derived from the elements of impedance tensor based on rotation criterion proposed by Swift (1967). It can be seen that the oscillating pattern in the far-field zone is uniform in the quadrant and the period of oscillation widening as increasing offset, clearly demonstrates the propagation feature of the radiation field at earth surface. The amplitude of the oscillation is stable at range of  $\pm 22.5^\circ$  and distinguishable even at large offset.

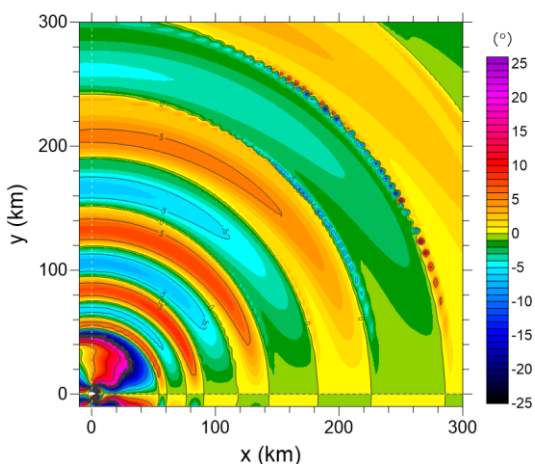


**Figure 5.** Contour plot of  $\theta_p$  at 100Hz in the x-y plane under excitation of an inclined electric dipole source in a five-layer earth.

It can be seen from the analysis of the above simulations that the anomalies produced by electric dipole in earth for this frequency band are characterized by sharp increase of the apparent resistivities and tipper, large amplitude of variation of  $\theta_p$  in the near-field zone; and typical radiation pattern of oscillating variations of amplitude and widen spatial period in far-field zone. This indicates that the SEM anomaly in terms of MT transfer function can be identified from observed MT responses if the radiation is strong enough.

### OBSERVED EXAMPLES

On May 18, 2016, an M5.0 magnitude earthquake occurred in Yunlong, Yunnan, with its epicenter located at  $26.10^\circ\text{N}$  and  $99.53^\circ\text{E}$ , and focal depth ranging from 3~17 km. On March 27, 2017, an M5.1 earthquake occurred in Yangbi, with its epicenter located at  $25.89^\circ\text{N}$ ,  $99.80^\circ\text{E}$ , and at depth of approximately 12 km. Figure 6 shows the epicenter and aftershock zone (light red area) of these two earthquakes, as well as the relative positions of the Dali and Lijiang MT stations near the earthquake area. The Dali Station is approximately 82.93km from the Yunlong epicenter and 47.18 km from the Yangbi epicenter. Lijiang Station is about 127.88km away from the Yunlong epicenter and 143.12km from the Yangbi epicenter.

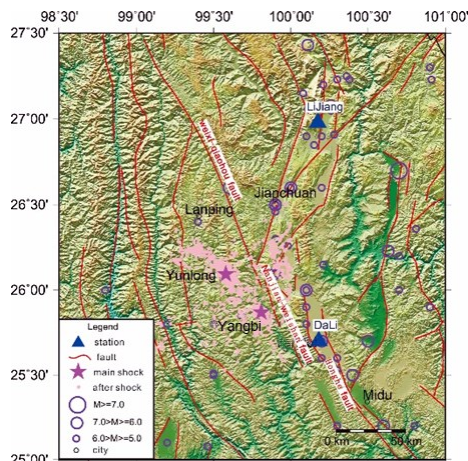
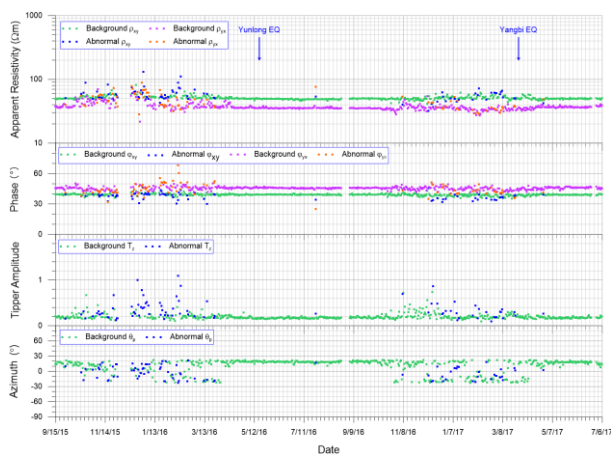


**Figure 6.** The epicenters of the Yunlong and Yangbi earthquakes, and location of Dali and Lijiang MT station.

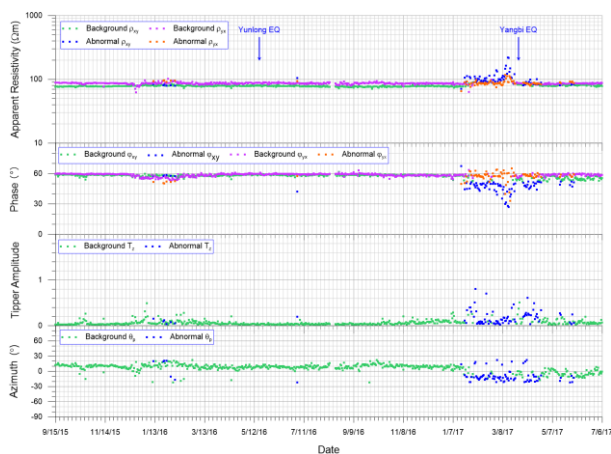
Over an extended observation period preceding the Yunlong and Yangbi earthquakes, the Dali and Lijiang stations recorded notable anomalies. Through long-term statistical averaging of observed data, background field information with high reliability can be obtained. Responses deviated from the background field by certain amplitude can be identified as responses containing SEM anomalies.

Figure 7 shows the temporal variations of the

apparent resistivity, impedance phase, tipper amplitude and azimuth of electric principal axis ( $\theta_p$ ) at 98 Hz, recorded by the Dali station over time period from September 15, 2015 to July 6, 2017. Corresponding result from Lijiang station is given in Figure 8. These plots reveal that, during quiescent periods, the apparent resistivity and phase for two polarization modes exhibit relative stability, as indicated by the background values. In contrast, the period leading up to the earthquakes is characterized by significant disturbances in all parameters, as denoted by the abnormal values. This pattern suggests that the anomalies, potentially indicative of seismic activity, are present within a specific time range.



**Figure 7.** Variations of apparent resistivity, phase, tipper and azimuth at the Dali station for time period of 9/15/2015~7/6/2017.



**Figure 8.** Variations of apparent resistivity, phase, tipper and azimuth at the Lijiang station for time period of 9/15/2015~7/6/2017.

### CONCLUSION

Using transfer functions and derived parameters from MT data to identify and extract SEM anomaly have following advantages: (1) Ratio of the mutually orthogonal electric and magnetic field is used to obtain the electric impedance of the earth

and then the apparent resistivity and impedance phase. Thus the influence of earth magnetic field variations can be automatically eliminated. (2) Reliable regional background resistivity information at different depths can be obtained from long-term observation by the network, which is convenient for identifying and extracting SEM anomalies. (3) The parameter  $\theta_p$  shows good feature of uniform radiation pattern and large stable amplitude oscillating variations, and could be an important indicator for SEM identification.

This study has demonstrated the potential of using subsurface electric dipole simulations for SEM radiation analysis, offering a feasible approach for the prediction and understanding of seismogenic zones by SEM anomalies.

### ACKNOWLEDGEMENT

The authors would like to express gratitude to the National Natural Science Foundation of China for supporting of project No. 41574064.

### REFERENCES

- Bastani M, Pedersen LB (2001) Estimation of magnetotelluric transfer functions from radio transmitters. *Geophysics* 66: 1038–1051
- Chen X (2003) New forward and inversion algorithms and a visual integrated system for MT data. PhD thesis, Institute of Geology, China Seismological Bureau, Beijing
- Hu KY, Hu WB, Huang QH (2023) Electromagnetic fields excited by arbitrarily orientated dipoles in horizontally layered earth. *Chin J Geophys*, 66: 3290–3301
- Parkinson WD (1959) Direction of rapid geomagnetic fluctuations. *Geophys J R astr Soc* 2, 1-14
- Swift CM (1967) A magnetotelluric investigation of an electrical conductivity anomaly in the southwestern United States. PhD thesis, Massachusetts Institute of Technology, Cambridge